

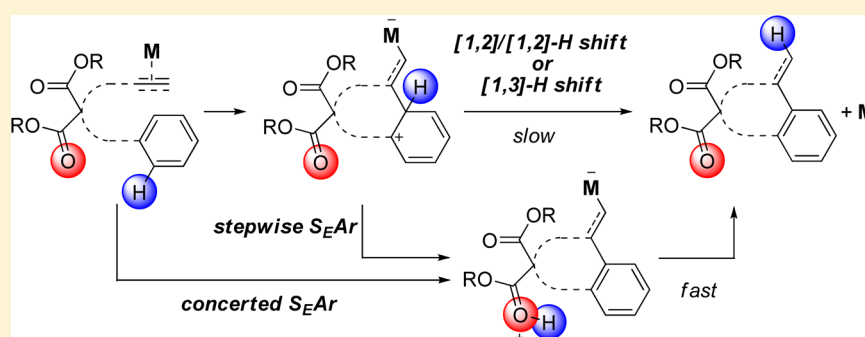
Non-Innocent Behavior of Substrate Backbone Esters in Metal-Catalyzed Carbocyclizations and Friedel–Crafts Reactions of Enynes and Arenynes

Bastien Michelet,[†] Guillaume Thiery,[†] Christophe Bour,[†] and Vincent Gandon^{*,†,§}

[†]ICMMO (UMR CNRS 8182), Université Paris-Sud, Bâtiment 420, 91405 Orsay cedex, France

[§]Institut de Chimie des Substances Naturelles, CNRS, Avenue de la Terrasse, 91198 Gif-sur-Yvette Cedex, France

S Supporting Information

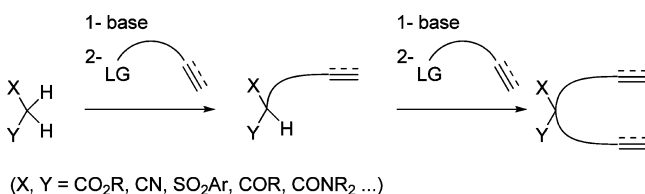


ABSTRACT: On the basis of DFT computations and experimental results, we show that the presence of the ester group in the backbone of organic substrates can influence the mechanism of metal-catalyzed carbocyclization reactions. The non-innocent role of the ester functionality in lowering the activation barrier of the key step of the gallium- and indium-catalyzed cycloisomerization of 1,6-enynes is revealed. In the case of the gallium-catalyzed hydroarylation of arenynes, the esters in the tether can deprotonate the Wheland intermediate, thus avoiding more energetically demanding [1,3]- or [1,2]/[1,2]-H shifts. As for the gallium-catalyzed Friedel–Crafts alkylation, an unusual concerted S_EAr mechanism involving the esters has been calculated. Lastly, computations evidence that the ester group of methyl propiolates enables a divergent mechanism in the platinum-catalyzed intramolecular hydroarylation.

1. INTRODUCTION

The synthesis of polyunsaturated substrates for metal-catalyzed reactions such as cycloisomerizations, metatheses, cycloadditions, etc., typically starts from an active methylene compound which is sequentially functionalized under basic conditions to form enynes, diynes, dienes, arenynes, etc. (Scheme 1). The electron-withdrawing

Scheme 1. Synthesis of Polyunsaturated Precursors from Active Methylene Compounds

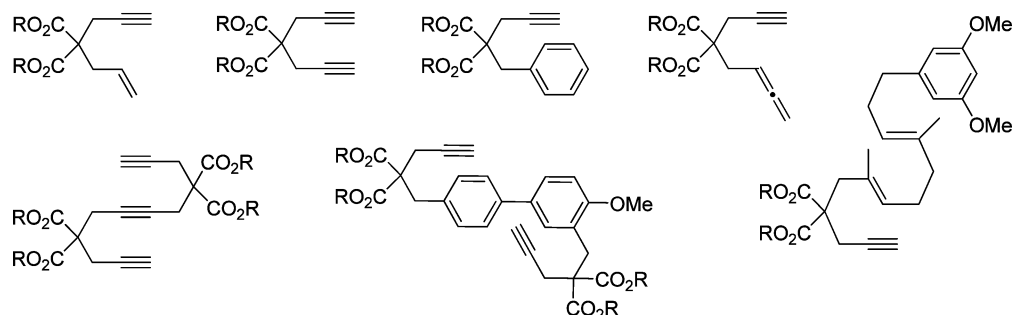
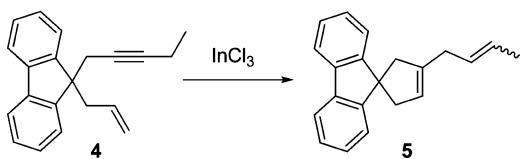
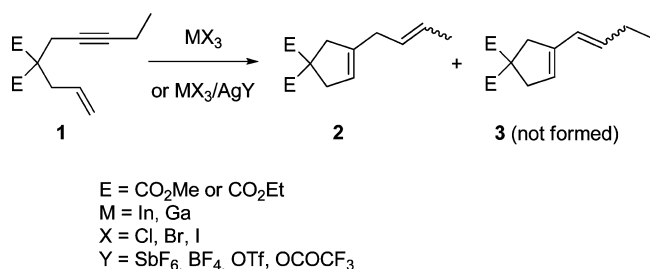


groups of the starting active methylene compound usually remain as part of the tether between the unsaturated C–C bonds, and their presence is well-tolerated in most cases.

For instance, countless substrates for metal-catalyzed reactions have been straightforwardly constructed by malonic ester synthesis (Chart 1).

The ease and versatility of this synthetic approach is not its only advantage. It is also well-established that the *gem*-disubstitution of the tether accelerates cyclization steps by Thorpe–Ingold or reactive rotamer effects.¹ One could also envisage that the presence of functional groups in the tether influences the elementary steps of a catalytic cycle in other ways. As they are at the same time electron-withdrawing groups and electron donors through their heteroatom lone pairs, they could possibly exert long-range inductive effects, stabilize charges, establish stabilizing noncovalent interactions, capture protons, etc. Some of these aspects are well-known in biology or sugar chemistry for instance, but they have been much less studied in the context of metal-catalyzed reactions. On the basis of DFT calculations, we show in this article that the *gem*-diester in the tether can provide more than a mere kinetic *gem*-disubstituent effect in gallium(III)- and indium(III)-catalyzed C–C bond forming reactions by serving as proton shuttle. In particular, an overlooked base-effect in Friedel–Crafts reactions leading to stepwise or concerted S_EAr pathways is discussed. We finally broaden the discussion to the case of a single ester substituent

Received: September 2, 2015

Chart 1. Examples of Substrates Used in Metal Catalysis Displaying a *gem*-Diester in the TetherScheme 2. Ga(III)- and In(III)-Catalyzed Cycloisomerization of Enynes **1** and **4**

47 located at the reactive alkyne unit of a substrate under platinum(II)
 48 catalysis and show that its presence can set up a new mechanistic
 49 scenario.

2. RESULTS AND DISCUSSION

50 **2.1. Ga(III)- and In(III)-Catalyzed Cycloisomerization of**
 51 **1,6-Enynes.** The metal-catalyzed cycloisomerization of enynes
 52 and related compounds is a well-established strategy for the rapid
 53 increase of the molecular complexity from simple substrates.²
 54 While a variety of transition-metal complexes can be used as
 55 catalysts for this reaction, simple salts derived from polarizable
 56 main group elements are also efficient, notably gallium and
 57 indium halides.³ In this section, we briefly reinvestigate part of a

previously reported computational study in which the struc-
 58 ture of the enynes has been simplified by removing the *gem*-
 59 disubstituent in the tethers.

In a series of recent papers, Yu et al. used a combined theo-
 61 retical and experimental approach to identify the real catalytic
 62 species in GaX_3 - and InX_3 -catalyzed cycloisomerization of 1,6-
 63 enynes.⁴ A large body of their work relies on the reactivity of the
 64 *gem*-diester tethered 1,6-enyne **1** which was previously shown by
 65 Miyanahana and Chatani to transform into the 1,4-diene **2** (*E/Z* 66
 mixture) exclusively in the presence of a catalytic amount of
 67 InCl_3 , and not into the conjugated diene **3** (Scheme 2).⁵ Starting
 68 from the postulate that almost all catalysts give conjugated dienes
 69 with 1,6-enynes except InCl_3 , Yu et al. decided to study this
 70 reaction in detail so as to elucidate the origin of this peculiarity.
 71 The formation of **2** as a sole product could be reproduced with
 72 GaCl_3 , GaBr_3 , InBr_3 , InI_3 , as well as with InCl_3/AgY mixtures
 73 ($Y = \text{SbF}_6, \text{BF}_4, \text{OTf, OCOF}_3$). The fluorene derivative **4** was
 74 also tested and gave rise to the nonconjugated product **5** with
 75 InCl_3 as catalyst.

A neutral and a cationic pathway was considered to account for
 77 the selective formation of the nonconjugated diene. A simplified
 78 overview of the mechanism limited to the most stable *trans*-
 79 isomers of **D**, **E**, **H**, and **I** is shown in Scheme 3. In the neutral
 80 pathway, enyne **1** forms complex **A** after coordination of MX_3 to
 81 the $\text{C}\equiv\text{C}$ bond. Nucleophilic attack of the $\text{C}=\text{C}$ bond provides
 82 the nonclassical carbocationic species **B** (depicted here as a
 83 chosen resonance form instead of the more abstruse resonance
 84 hybrid),^{3b} which then rearranges into the key intermediate **C**.
 85 The latter is the precursor of the isolated product after selective
 86 [1,2]-H migration of Hb (see complex **D**). That of Ha on the
 87

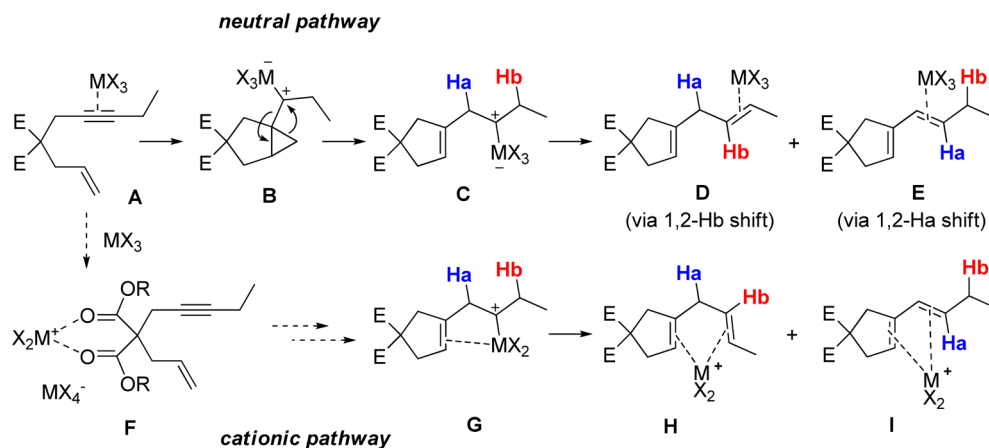
Scheme 3. Possible Mechanistic Pathways of the Ga(III)- and In(III)-Catalyzed Cycloisomerization of Enyne **1**

Table 1. Free Energies of Activation (kcal/mol) of the Key Step of the Ga(III)-Catalyzed Cycloisomerization of a Model 1,6-Enyne

entry	theory level ^a	TSa-GaCl ₃	TSb-GaCl ₃	TSa-GaCl ₂ ⁺	TSb-GaCl ₂ ⁺
1	B3LYP/BS1	7.7	9.7	8.3	5.2
2	B3LYP/BS2	9.1	10.8	6.4	3.0
3	M06-2X/BS3	9.0	9.6	4.4	1.9

^aBS1: LANL2DZ+ECP (Ga), 6-31G(d) (other elements), values of entry 1 taken from the Supporting Information of ref 4c; BS2:6-31G(d) (all elements); BS3:6-311+G(d,p) (all elements).

Table 2. Ga(III)-, In(III)-, and Au(I)-Catalyzed Cycloisomerization of Enyne 1

entry	catalyst	T (°C)	t (h)	E:Z ^a	yield ^b
1	[IPr-GaCl ₂][Al(pftb) ₄] ^c	80	4	8:1	32 (97)
2	[IPr-InBr ₂][Al(pftb) ₄] ^c	80	2	4:1	42 (92)
3	[Ph ₃ PAu][SbF ₆] ^d	20	1	4:1	50 (99)

^aDetermined by GLC analysis. ^bCorrected yield of **2** admixed with some unreacted **1**, conversions are indicated in parentheses. ^cGenerated in situ from IPr-MX₃ (5 mol %) and [Ag][Al(pftb)₄]¹¹ (7 mol %). ^dGenerated in situ from Ph₃PAuCl (5 mol %) and AgSbF₆ (7 mol %).

88 other hand furnishes the unobserved conjugated product (see
89 complex E).

In the papers of Yu et al., calculations were carried out using 90
the B3LYP functional, the LANL2DZ+ECP basis set for In or 91
Ga, and the 6-31G(d) basis set for other elements (noted BS1 in 92
Table 1). On the basis of these DFT computations, the neutral 93
pathway was ruled out. For instance, with GaCl₃, calculations 94
predict the wrong isomer E (see TSa-GaCl₃ vs TSb-GaCl₃ in 95
Table 1, entry 1).⁶ The migration of Ha through TSa-GaCl₃ 96
would require 7.7 kcal/mol of free energy of activation, while that 97
of Hb through TSb-GaCl₃ would require 9.7 kcal/mol. We have 98
reproduced these calculations at a slightly different level of theory 99
and reached the same conclusions (entry 2, B3LYP/6-31G(d) 100
for all atoms (BS2)). 101

A cationic scenario was then envisaged by Yu et al. They 102
suggested that MX₃ salts could react with the solvent or the 103
substrate to form MX₂⁺ ions. An ion peak corresponding to 104
[InCl₂+2]⁺ could be detected by ESI-HRMS analysis of a reac- 105
tion mixture comprising 150 mol % of InCl₃, enyne **1**, and aceto- 106
nitrile. The proposed structure corresponds to F in Scheme 3, in 107
which MX₂⁺ is coordinated to the ester groups of the tether of the 108

Table 3. M06-2X Free Energies of Activation (kcal/mol) of the Key Step of the MCl₃-Catalyzed Cycloisomerization of Enynes 4 (left) and 1 (right)

entry	basis set ^a	TSa'-InCl ₃	TSb'-InCl ₃	TSa''-GaCl ₃	TSb''-GaCl ₃	TSa''-InCl ₃	TSb''-InCl ₃
1	BS3	—	—	— ^b	4.7 [6.9] ^c	—	—
2	BS4	10.2	7.2	—	—	— ^b	3.6 [6.2] ^c

^aBS3: 6-311+G(d,p) (all elements); BS4: 6-311+G(d,p) (C, H, O, Cl), LANL2DZ+ECP (In). ^bNot found. ^cFree energy of activation of the unassisted 1,2-Hb shift.

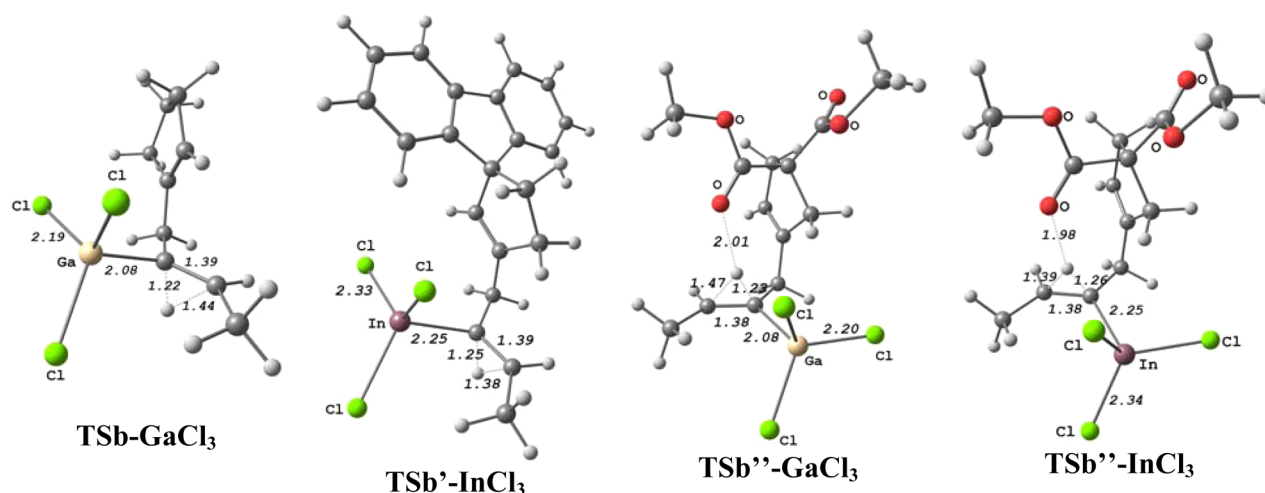
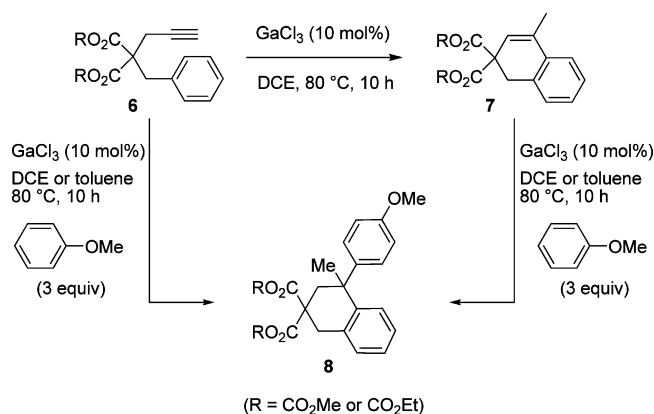


Figure 1. Selected geometries of the most stable 1,2-Hb migration transition states (distances in Å).

Scheme 4. Ga(III)-Catalyzed Hydroarylation/Friedel–Crafts Tandem of Arenyne 6



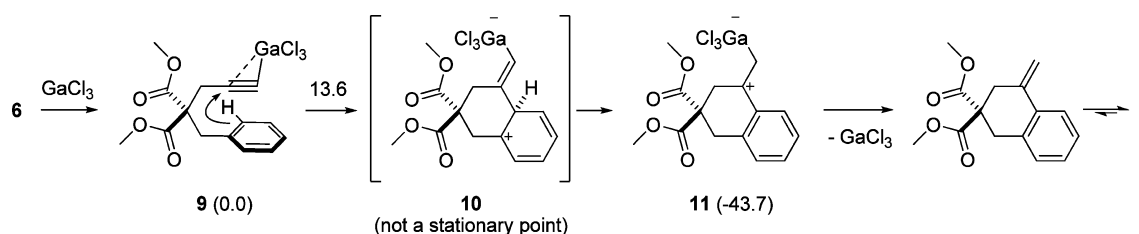
enyne. However, acetonitrile is a solvent in which the reaction cannot occur catalytically.^{4a,7} Nevertheless, the possibility that MX_2^+ could be the actual active species was checked computationally by Yu et al. With GaCl_2^+ instead of GaCl_3 , the computations predicted the experimentally observed nonconjugated product as the preferred one (see TSa-GaCl_2^+ vs TSb-GaCl_2^+ in Table 1, entry 1). Again, we reached the same conclusions with BS2 (entry 2). It was suggested that the migration of Ha or Hb is encouraged by the electronic effect of the nearby cyclopentene or methyl group. Since the cyclopentene is electron-rich, the migration of Ha should be always favored, as with GaCl_3 for instance. Yet, since GaCl_2^+ displays two vacant orbitals instead of one in GaCl_3 , complexation of the $\text{C}=\text{C}$ bond in the key intermediate becomes possible. This electron depletion renders

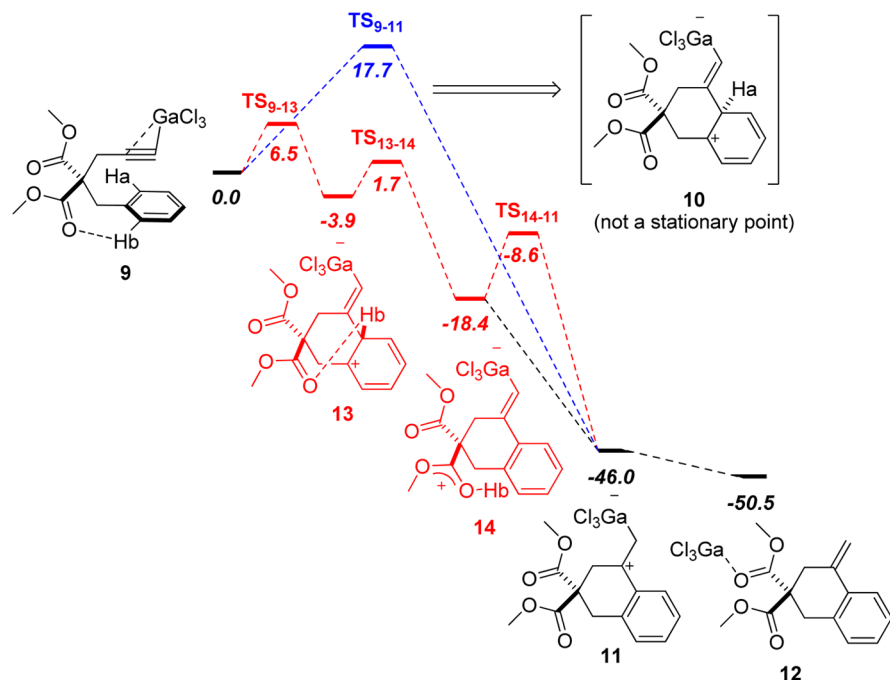
the terminal methyl group electron-rich, hence the preferred migration of Hb with GaCl_2^+ .

Yu et al. now recommend the use of 1,6-enynes as mechanistic probes to identify the real active species when GaX_3 or InX_3 salts are used as catalysts.^{4c} If the reaction of 1 gives 2, then the active species should be GaX_2^+ or InX_2^+ , and not GaX_3 or InX_3 . On the other hand, if the conjugated product 3 is obtained, then only the neutral pathway could explain its formation. Our research group has specialized in the use of neutral and cationic gallium and indium complexes in molecular catalysis.⁸ In particular, we have developed the synthesis of complexes of type $[\text{IPr} \cdot \text{MX}_2]^+[\text{Y}]^-$ ($\text{M} = \text{Ga}, \text{In}$; $\text{X} = \text{Cl}, \text{Br}, \text{I}$; $\text{IPr} = 1,3\text{-bis}(2,6\text{-diisopropylphenyl})\text{-imidazol-2-ylidene}$; $\text{Y} = \text{weakly coordinating anion}$). These complexes can be isolated or generated in situ from $\text{IPr} \cdot \text{MX}_3$ and AgY . Since they display a single coordination site, we reasoned that they should be able to imitate the behavior of monocoordinating transition-metal fragments and yield the conjugated product. Surprisingly, these species also gave rise to 2 selectively from 1 (Table 2, entries 1 and 2). After realizing that actually no report mentioned the formation of 2 or 3 by transition-metal-catalyzed cycloisomerization of 1,⁹ we tested it under $\text{Au}(\text{I})$ catalysis¹⁰ and obtained again product 2 (entry 3). However, with $\text{IPr} \cdot \text{MX}_2^+$ or Ph_3PAu^+ fragments, the coordination of the cyclopentene moiety to the metal center is unlikely.

To address this discrepancy, we decided to test a different level of theory and then to take the *gem*-diester substitution into account. It is well-established that while the B3LYP functional usually lead to reliable geometries, better energies can be obtained with the Minnesota series of functionals.¹² Among them, the M06-2X performs very well for main group chemistry and noncovalent interactions.¹³ The free energies shown in Table 1,

Scheme 5. Previously Reported Relative Free Energies (ΔG_{298} , kcal/mol) for the Hydroarylation of 6 at the B3LYP/BS1 Level^{8a} (a Value over an Arrow Corresponds to the Relative Free Energy of a Transition State)



Scheme 6. Free Energy Profile of the Hydroarylation of Arenyne 6 (ΔG_{298} , kcal/mol) at the M06-2X/BS3 Level

entry 3, have been obtained at the M06-2X/6-311+G(d,p) level. While the preference for the nonconjugated product remains clear with GaCl_2^+ , it is no longer obvious that GaCl_3 would encourage the selective formation of the conjugated one, as the formation of products is expected to take place at very similar energy costs. Thus, the choice in the level of theory seems critical.

In fact, the model enyne used by Yu et al. has not been tested experimentally.¹⁴ It does not display the esters or the biphenyl group of **1** or **4**. Thus, we decided to use the real *gem*-diester tethered enyne **1** ($\text{E} = \text{CO}_2\text{Me}$) and the fluorene derivative **4** in the computations.¹⁵ With the latter (Table 3), both BS3 (entry 1) and BS4 (entry 2), which is the same as BS3 with the LANL2DZ +ECP basis set for In, predict the correct isomer without invoking InCl_2^+ as active species. Moreover, with enyne **1**, only the formation of the nonconjugated diene could be modeled with $\text{M} = \text{GaCl}_3$ (entry 1) and $\text{M} = \text{InCl}_3$ (entry 2).

Interestingly, the geometry of the most stable transition states leading to the nonconjugated product varies greatly when esters are present in the tether (Figure 1). Alkane and fluorene tethered systems adopt a *trans* relationship between the migrating hydrogen and the cyclopentene framework (see TSb-GaCl_3 and TSb-InCl_3). On the other hand, a *cis* relationship is found in the *gem*-diester tethered transition states. The corresponding *cis* complexes have been computed as well and are significantly less stable by ~ 2.5 kcal/mol (see values in brackets in Table 3). The stabilization observed in the *cis* series is due to an interaction between the migrating hydrogen and one carbonyl oxygen. In $\text{O}\cdots\text{H}$ area, inspection of the maximum electron density reveals quite strong hydrogen bonds ($\rho_{\text{max}} = 0.019$ and $0.023 \text{ e}^- \text{\AA}^{-3}$, respectively, for the Ga and In complexes). Thus, one ester group assists the [1,2]-H shift.

Our calculations on the “real” fluorene and *gem*-diester tethered systems show that there is no need to coordinate the $\text{C}=\text{C}$ bond of the cyclopentene moiety to favor the migration of Hb and obtain the nonconjugated product thereof. This rapid re-examination of a previously studied reaction has revealed that the choice of the level of theory is critical and that oversimplifying

the substrate in such computations can lead to conclusions at odds with experimental results. It has also shown that the presence of esters in the tether can favor specific conformations due to the presence of basic sites and lower activation barriers. Since there is at present no reason to invoke MX_2^+ ions as active species in MX_3 -catalyzed transformations ($\text{M} = \text{Ga}, \text{In}$), GaCl_3 has been used in the next section.

2.2. GaCl_3 -Catalyzed Friedel–Crafts Reactions. It is well-established that Group 13 salts are exquisite catalysts for Friedel–Crafts reactions.¹⁶ Among them, gallium(III) halides are often more efficient and safer catalysts than the corresponding aluminum salts.¹⁷ Although a few computational studies on Group 13 halide-catalyzed Friedel–Crafts reaction of simple compounds (benzene, acetyl chloride, 2-chloropropane, etc.) have been reported,¹⁸ they reveal that the intimate mechanism is actually far more complex than anticipated. In particular, the deprotonation steps are not the same in AlCl_3 -catalyzed Friedel–Crafts acylation and alkylation.^{18d} In both cases, the driving force to deprotonate the Wheland intermediate is the establishment of a strong hydrogen bond with the chlorine-bridged counterion Al_2Cl_7^- which plays the role of base. However, for the alkylation, an Al_2Cl_7^- -assisted [1,2]-H shift actually precedes the deprotonation. For Group 13 halide-catalyzed hydroarylation of alkynes, alkenes, and allenes, theoretical studies are also scarce, and the deprotonation has not been studied.^{8a,19} In this section, we investigate the mechanism of the GaCl_3 -catalyzed hydroarylation of 1,6-arenynes and the subsequent bimolecular Friedel–Crafts reaction of the resulting dihydronaphthalenes with anisole.

It was previously reported that *gem*-diester tethered arenynes such as **6** undergo GaCl_3 -catalyzed hydroarylation in 1,2-dichloroethane (DCE) at 80°C to give bicyclic compounds such as **7** (Scheme 4).^{3a} When the reaction of **6** or **7** is carried out in DCE or toluene at 80°C in the presence of an aromatic nucleophile such as anisole, the adduct **8** is obtained.

We have previously studied the hydroarylation mechanism by means of DFT computations at the B3LYP/LANL2DZ +ECP(Ga),6-31G(d) (other elements) level, including solvent

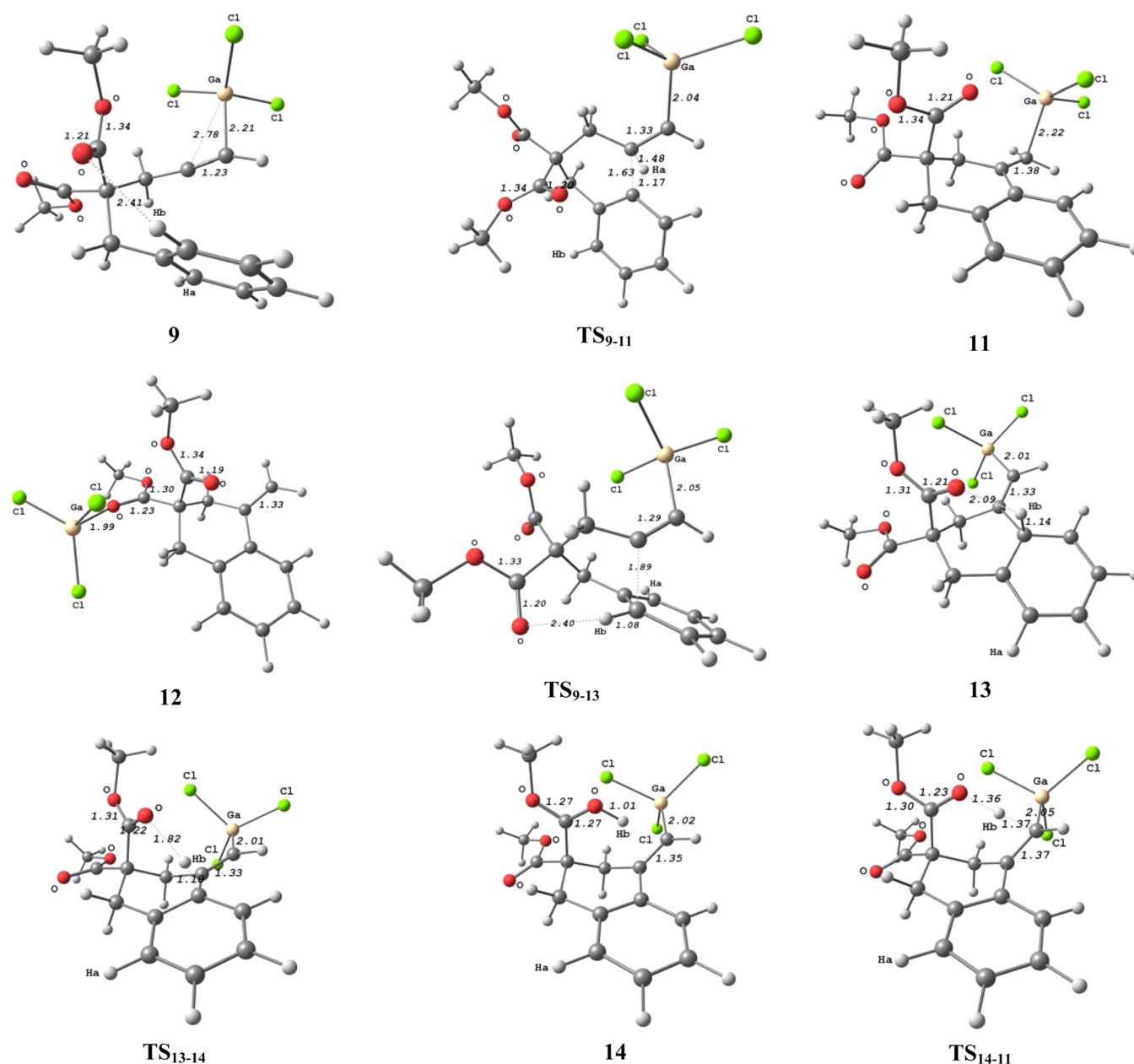
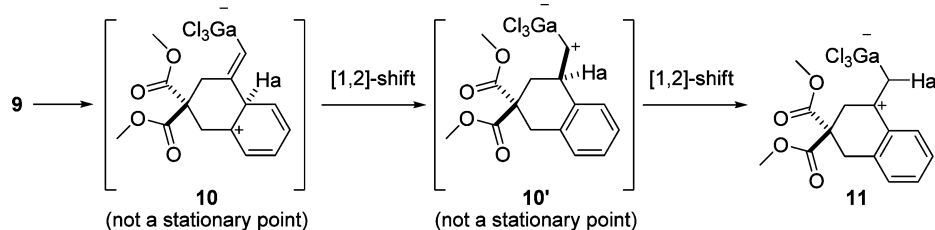


Figure 2. Geometries of the computed species shown in Scheme 6 (distances in Å).

Scheme 7. Resemblance Between TS_{9-11} and the Fictive $TS_{10-10'}$

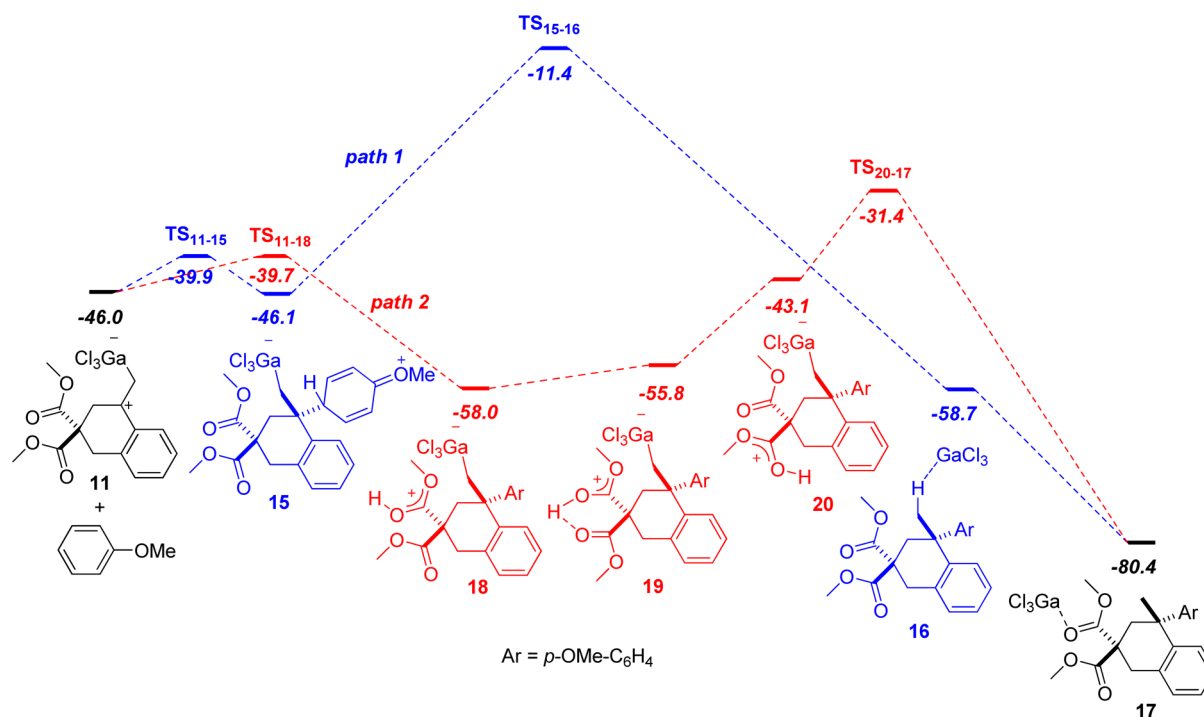


228 correction for DCE.^{8a} These results are summarized in
 229 Scheme 5. The coordination of the $C\equiv C$ bond of **6** to
 230 give **9** triggers the nucleophilic attack of the benzene moiety
 231 to give **11** directly with a release of 43.6 kcal/mol of free
 232 energy. The transition state lies 13.6 kcal/mol above **9**. The
 233 expected Wheland intermediate **10** did actually not con-
 234 verge. Dissociation of $GaCl_3$ and thermodynamically driven

exocyclic/endocyclic shift of the $C=C$ bond provides **7**.
 The subsequent bimolecular Friedel–Crafts step has not been
 studied computationally.

We decided to reinvestigate the hydroarylation mechanism
 and to study the Friedel–Crafts step at the M06-2X/BS3 level
 (Scheme 6). To allow comparison with our previous results,
 solvent correction for DCE was included.

Scheme 8. Free Energies Profile of the Friedel–Crafts Step of the Tandem Transformation of Arenyne 6 (ΔG_{298}^\ddagger , kcal/mol) at the M06-2X/BS3 Level



In the most stable isomer of **9**, the two carbonyls adopt an *anti* relationship (Figure 2). Therefore, the *ortho* hydrogens Ha and Hb of the benzene moiety are not equivalent, and significant electron density indicative of a noncovalent interaction was found between Hb and the nearby carbonyl oxygen ($O\cdots Hb$ 2.41 Å, $\rho_{\max} = 0.011 \text{ e} \cdot \text{\AA}^{-3}$). The attack of the benzene carbon bearing Ha requires 17.7 kcal/mol of free energy of activation and leads, as in the B3LYP case mentioned above, to **11** without intermediate. This step is strongly exergonic by 46.0 kcal/mol. Migration of GaCl_3 from the carbon to one carbonyl oxygen results in a further release of 4.5 kcal/mol. If the Wheland intermediate had converged, its transformation into **11** would have been the result of two suprafacial [1,2]-H shifts instead of a symmetry forbidden [1,3]-H shift (Scheme 7).¹⁹ Inspection of the transition vector of TS_{9-11} actually shows that it corresponds to the first [1,2]-H shift. Yet neither **10** nor **10'** are stable and collapse to **11** in the forward direction and to **9** in the backward direction.

The attack of the carbon bearing Hb proceeds quite differently. It leads to the Wheland intermediate **13** which is formed in an exergonic fashion ($\Delta G_{298} = -3.9 \text{ kcal/mol}$) through a transition state that lies only 6.5 kcal/mol above **9**. In **13**, the $O\cdots Hb$ distance is only 2.09 Å and ρ_{\max} increases to $0.019 \text{ e} \cdot \text{\AA}^{-3}$. Migration of Hb to O is achieved through a low-lying transition state ($\Delta G_{298}^\ddagger = 5.6 \text{ kcal/mol}$ for this step) and **14** is formed in an appreciably exergonic fashion ($\Delta G_{298} = -14.5 \text{ kcal/mol}$). The shift of Hb from O to the carbon bearing the gallium atom is also straightforward as far as the free energy of activation is concerned ($\Delta G_{298}^\ddagger = 9.8 \text{ kcal/mol}$), and it is strongly exergonic ($\Delta G_{298} = -27.6 \text{ kcal/mol}$).^{20,21}

The Friedel–Crafts reaction was studied next (Scheme 8 and Figure 3). Here again, we found two pathways to reach compound **8** shown in Scheme 4 (i.e., **17** in Scheme 8 with GaCl_3 coordinated to one carbonyl oxygen of **8**). The first one does not involve the esters (path 1). Complex **11** and anisole

transform through a relatively low-lying transition state ($\Delta G_{298}^\ddagger = 6.1 \text{ kcal/mol}$) into the Wheland intermediate **15** in a virtually athermic fashion. A proton transfer giving rise to the σ -complex **16**,²² and then the O-coordinated complex **17** was computed. Despite the downhill nature of this sequence ($\Delta G_{298} = -12.6 \text{ kcal/mol}$ to **16** and then -21.7 kcal/mol from **16** to **17**), the [1,3]-H shift requires a high free energy of activation of 33.9 kcal/mol.

Alternatively, **11** can react with anisole in a process which involves the simultaneous C–C bond formation and cleavage of the C–H bond (path 2). One carbonyl oxygen of **11** serves as base to deprotonate anisole which is found already aromatic in **18**. Concerted $\text{S}_{\text{E}}\text{Ar}$ mechanisms for arene sulfonation²³ and chlorination²⁴ have been computed and refute the traditional text-book perspective of Friedel–Crafts reactions systematically involving Wheland σ -complexes. However, the possibility of concerted Friedel–Crafts alkylation involving a three-centered transition state is unknown to us (Scheme 9).

The free energy of activation of the concerted $\text{S}_{\text{E}}\text{Ar}$ is virtually the same as the one to reach **15**. Isomers of **18** in which the proton is shared by the two carbonyl oxygen atoms (**19**) or is fixed at the one *cis* to the GaCl_3 fragment (**20**) were computed, yet they are less stable than **18**. Nevertheless, from **20**, oxygen-to-carbon migration can occur. The transition state of this proton-demetalation step lies much lower in free energy than the one from **15** to **16** (-31.4 vs -11.4 kcal/mol). Therefore, the ester-assisted addition of anisole to **11** is the most favorable pathway.

One could argue that the proton migration could take place in an intermolecular solvent-mediated fashion, yet the above reaction works equally well in toluene.^{8a} Another possibility would be a bimolecular process between two reaction intermediates; however, this scenario was ruled out by the study of the reactivity of a substrate that does not display hydrogen-bond-acceptor functionalities: the fluorene derivative **21** (Scheme 10). When submitted to GaCl_3 in DCE or toluene, the hydroarylation took place but not the Friedel–Crafts step.

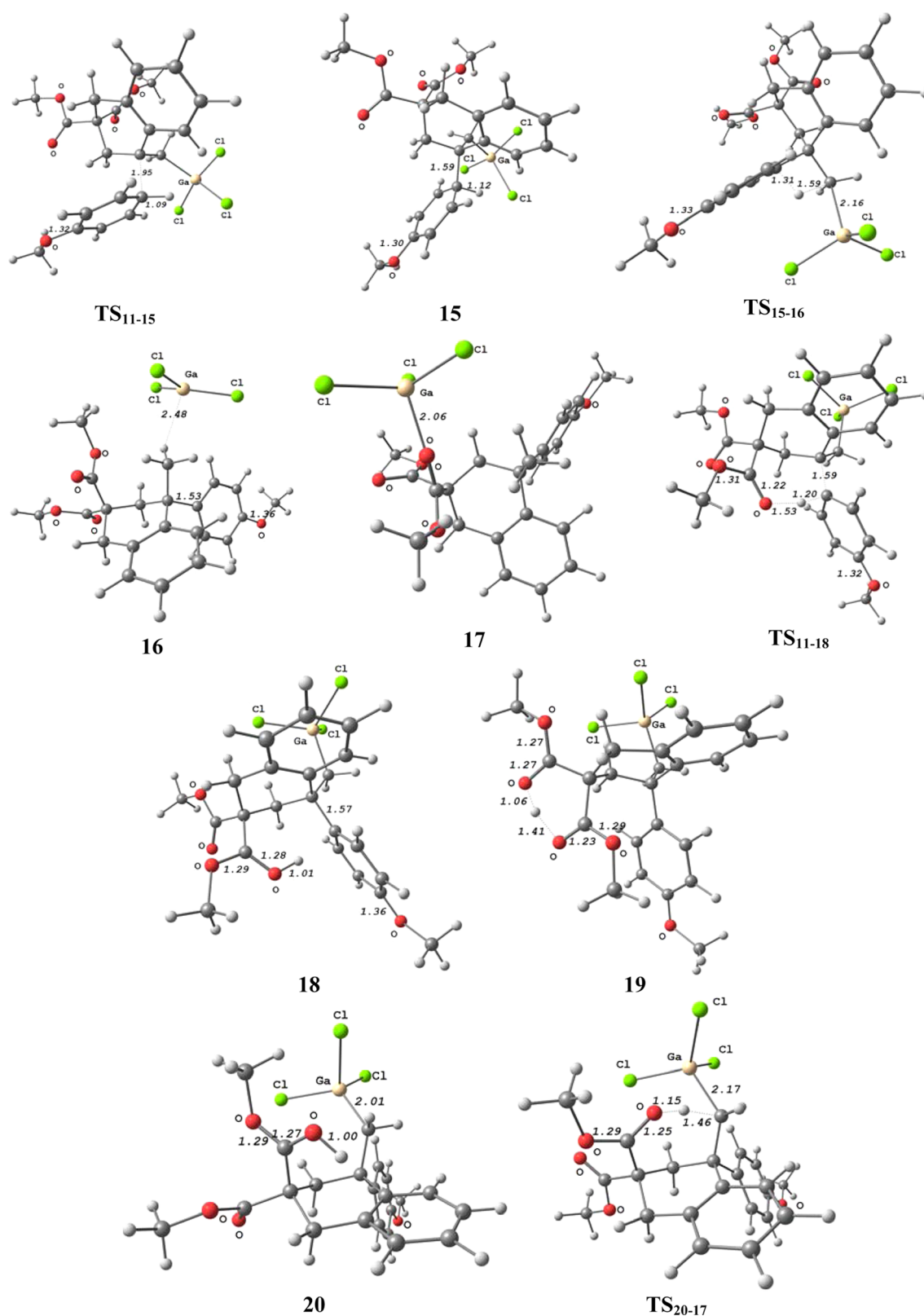
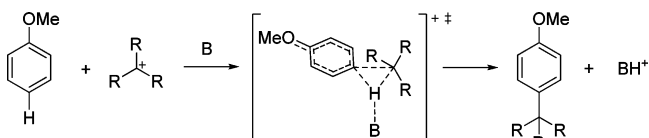


Figure 3. Geometries of the computed species shown in Scheme 8 (distances in Å).

Computations rationalize this feature (Scheme 11 and Figure 4). The hydroarylation proceeds in a concerted fashion through a low-lying transition state ($\Delta G_{298}^\ddagger = 8.5$ kcal/mol).²⁵ The formation of **25** is strongly exergonic ($\Delta G_{298} = -48.6$ kcal/mol). That of the Wheland intermediate **26** requires a modest free energy of activation

of 5.7 kcal/mol and is endergonic by 2.8 kcal/mol. Again, the protodemetalation step (**26** to **27** and then **28**), although strongly exergonic ($\Delta G_{298} = -9.2$ kcal/mol and then -25.2 kcal/mol) is compromised by a high activation barrier of 30.0 kcal/mol. Since there is no basic sites in the substrates, there is no alternative route.

Scheme 9. Possible Concerted Friedel–Crafts Alkylation



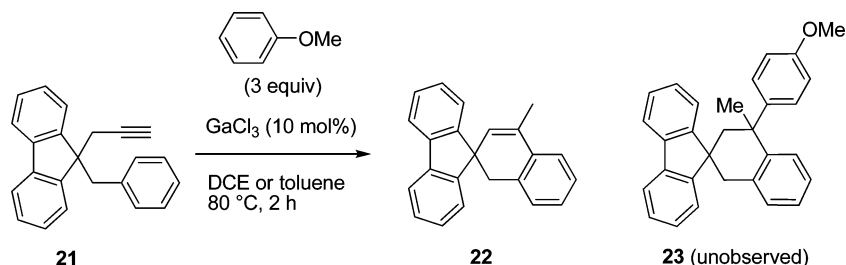
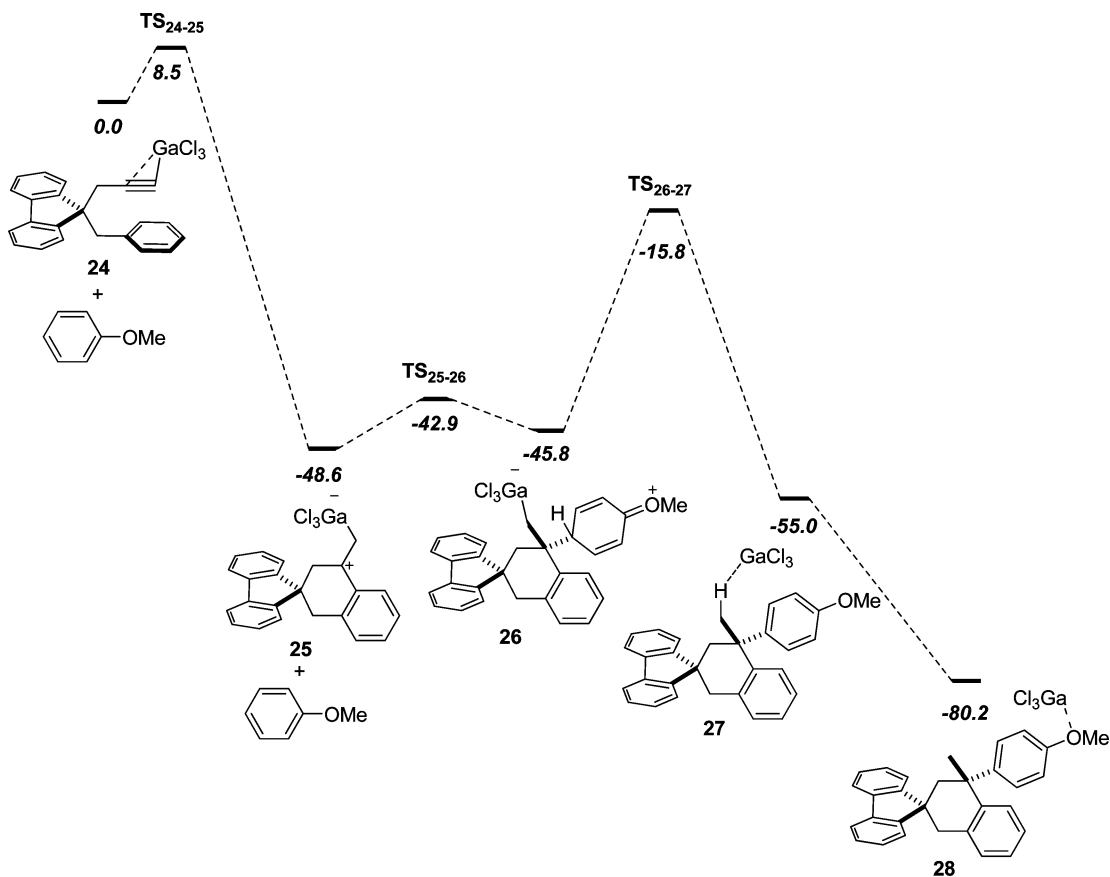
Even though the calculations presented in Sections 2.1 and 2.2 are restricted to Group 13 metal-catalyzed reactions involving *gem*-diester tethered substrates, there is no reason to believe that the conclusions reached would not apply to other kind of transformation involving a proton transfer, as long as a functional group such as an ester is well enough located to shuttle the migrating hydrogen. To address this issue, we have next studied a platinum(II)-catalyzed reaction in which the substrate does not display a *gem*-diester tether, but a simple ester substituent at the reacting alkyne unit of an arenynes.

2.3. PtCl₂-Catalyzed Hydroarylation of 1,6-Arenynes.

In this section, we turn our attention to the hydroarylation of biphenylacetylenes described by Fürstner²⁶ for the following reasons: (i) not only main group metal salts but also transition-metal complexes such as PtCl₂ are known to be active catalysts for this transformation; (ii) the cyclization of a substrate displaying a single ester group has been carried out; and (iii) the mechanism has already been studied by Soriano but the possibility of ester-assisted proton transfer has not been considered.¹⁹ In fact, the cyclization of such substrates can lead to fluorenes or phenanthrenes, the latter type being the major one when PtCl₂ is used as catalyst, except with an ester at the alkyne terminus as in 29 (Scheme 12). In this case, the fluorene derivative 30 is formed selectively as an *E/Z* mixture.

From B3LYP/LANL2DZ+ECP(Pt),6-31G(d) (other elements) computations used on a simplified model substrate, Soriano and Marco-Contelles proposed a mechanism involving a 5-*exo*-dig or a 6-*endo*-dig attack of the arene onto the complexed

Scheme 10. Ga(III)-Catalyzed Hydroarylation of Arenyne 21

Scheme 11. Free Energy Profile of the Hydroarylation/Friedel–Crafts Transformation of Arenyne 21 (ΔG_{298} , kcal/mol) at the M06-2X/BS3 Level

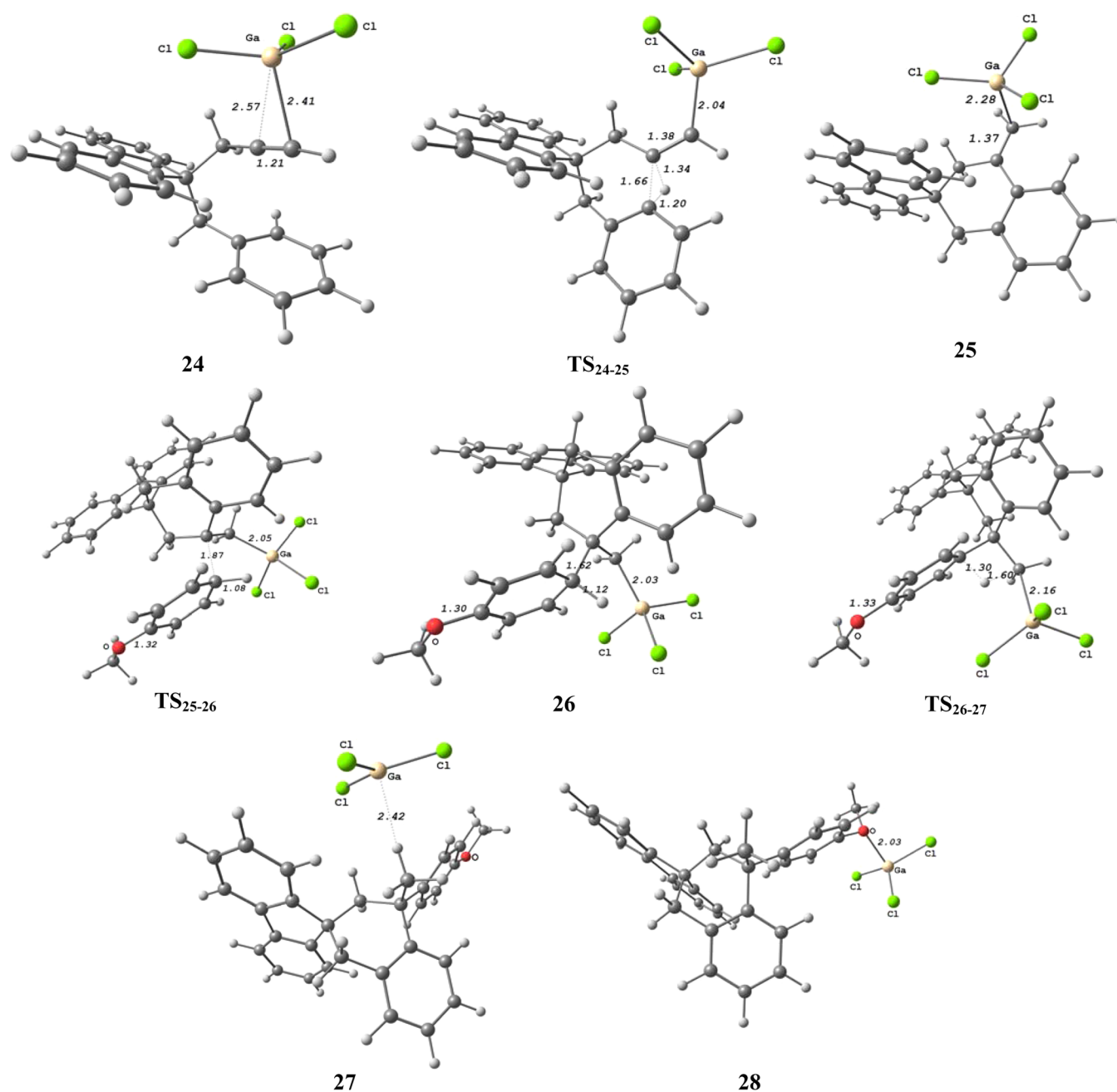
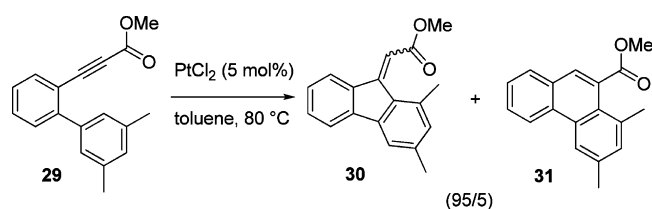


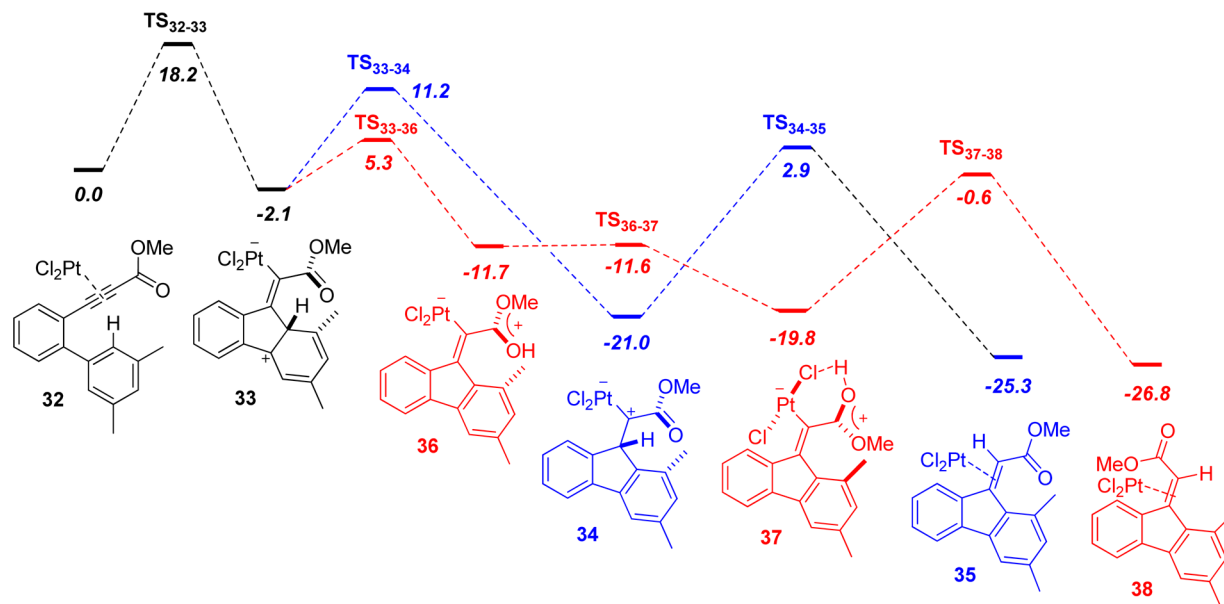
Figure 4. Geometries of the computed species shown in Scheme 11 (distances in Å).

Scheme 12. Platinum-Catalyzed Cycloisomerization of Compound 29



350 C≡C bond, followed by two [1,2]-H shifts. They showed that
 351 the reversal of selectivity between the 5-*exo* and the 6-*endo*
 352 pathways was due to the polarization of the C≡C bond induced
 353 by the ester. The preference for the 5-*exo*-dig cyclization was
 354 shown on the “real” substrate 29, but the [1,2]-H shifts were not

computed in this case. Intrigued by the proximity of the carbonyl
 group with the migrating proton in complex 33, we decided
 to compare the [1,2]-H shifts sequence with an ester-assisted
 proton transfer (Scheme 13 and Figure 5). From our part, we
 used the B3LYP/LANL2DZ+ECP(Pt),6-311+G(d,p) (other
 elements) level for the geometry optimizations and to get the
 thermal corrections to the free energies. We then carried out
 single point calculations using the M06 functional, the SDD basis
 set for Pt, and the 6-311+G(d,p) basis set for other elements. A
 barrier of 18.2 kcal/mol was computed for the transformation of
 starting complex 32 into the Wheland intermediate 33, which
 represents the rate-determining step. From 33, 13.3 kcal/mol of
 activation energy is required to give the platinum carbenoid 34.
 The second [1,2]-H shift leading to the complexed alkene 35 is
 achieved at a free energy cost of 23.9 kcal/mol. The entire
 sequence is downhill with a total exergonicity of 25.3 kcal/mol.

Scheme 13. Free Energy Profile of the Hydroarylation of Arenyne 32 (ΔG_{298} , kcal/mol) at the M06 Level

From 33, the capture of the proton proceeds straightforwardly through a 7.4 kcal/mol activation barrier. A virtually barrierless rotation of the protonated ester in 36 yields 37, which is greatly stabilized by an OH...Cl hydrogen bond. Protodemetalation finally takes place through a 20.4 kcal/mol activation barrier to give 38, which is actually the diastereomer of 35. Indeed, the migration of the proton to the metalated carbon atom requires rotation of the C=C bond. The overall 33 → 38 process is also downhill and is kinetically favored over the 33 → 35 pathway. Thus, the ester group at the alkyne enables a mechanistic alternative. It can serve as proton carrier to ensure the rearomatization of the Wheland intermediate and the protodemetalation step.

3. CONCLUSION

The above computations indicate that the ester functionality can play an active chemical role in metal-catalyzed carbocyclization and Friedel–Crafts reactions by shuttling protons from one place to another. In particular, a rare kind of concerted S_EAr where the ester functionality acts as base has been uncovered. While the ability of carbonyls to transfer hydrogens is well-known in the coordination sphere of a metal (for instance inner sphere pivalate-assisted concerted metalation deprotonation (CMD)),²⁷ it is overlooked in metal-catalyzed reactions occurring under substrate control.

4. EXPERIMENTAL SECTION

Computations. All the calculations were performed using the GAUSSIAN 09 software package.²⁸ For the study of gallium- and indium-catalyzed reactions, the structures were optimized and characterized to be energy minima (no imaginary frequency) or transition states (one imaginary frequency) at the M06-2X²⁹ level. The 6-311+G(d,p)³⁰ basis set (BS3) was used for C, H, N, Cl, O, and Ga, and the LANL2DZ+ECP³¹ basis set was used for In (BS4). The thermal corrections to free energies were carried out at 298.15 K and 1 atm using the M06-2X harmonic frequencies (ΔG_{298}). Solvent corrections to the free energies were obtained for DCE with the CPCM model.³² For the study of the platinum-catalyzed reaction, computations were carried out at the B3LYP³³ level using the LANL2DZ+ECP³¹ basis set for Pt and the 6-311+G(d,p)³⁰ basis set for the other elements. Single point calculations using the B3LYP optimized geometries were carried out with the M06²⁹ functional and a larger basis set of SDD³⁴ for Pt. The thermal

corrections to free energies were obtained at 298.15 K and 1 atm using the B3LYP harmonic frequencies (ΔG_{298}).

General Information. All reactions were performed in oven-dried flasks under argon atmosphere. Unless otherwise stated, commercially available reagents were used as received without further purification. Gallium and indium halides were obtained from a commercial source and used as received. Silver hexafluoroantimonate was purchased from a commercial source and used as received. DCE was distilled from calcium hydride and degassed by freeze–pump–thaw technique. Unless otherwise stated, products were purified by chromatography over silica gel. TLC plates were visualized by UV light (254 nm) and *p*-anisaldehyde staining. GC analysis was performed with a nonpolar column (15 m × 0.25 mm × 0.25 mm) NMR spectra were recorded on 360 and 300 MHz spectrometers. Chemical shifts are reported in parts per million (ppm). The spectra were referenced to the residual ¹H and ¹³C signals of the solvents as follows: CDCl₃ (¹H, δ = 7.27 ppm; ¹³C, δ = 77.0 ppm). Data are given in the following order: chemical shift, multiplicity (*s* = singlet, *d* = doublet, *m* = multiplet), coupling constant (*J*) in Hz and integration. Infrared spectra were recorded on a FTIR spectrometer (KBr pellets) and are reported in cm^{−1}. HRMS were performed by electrospray ionization using a qTOF mass spectrometer. IPr-GaCl₃,³⁵ IPr-InBr₃,³⁶ and [Ag][Al(pftb)₄]¹¹ were prepared following reported procedures. Enyne 1 was synthesized according to a previously described method.^{4a} Arenyne 6 was prepared following a reported procedure.^{8a,b} The synthesis and characterization of compounds 7 and 8 were previously reported by our team.^{8a} Arenyne 21 and cycloalkene 22 were also described previously.^{8b}

Procedures for the Cycloisomerization of Enyne 1. General Considerations. the substantial difference between conversions and isolated yields can be explained by polymerization occurring as side reactions. Thus, rinsing silica gel with Et₂O after flash chromatography leads to the recovery of the missing material as a very complex mixture. These complex mixtures were already observed by ¹H NMR analysis of the crude product before the purification step. Also, as Yu et al. have previously stated,^{4a} the generated dienes are stable on silica gel. Moreover, no other isomers arising from 1 could be observed by GC monitoring. The NMR spectra of 2 displayed in the Supporting Information were obtained from condition B as a representative outcome of a main-group metal-catalyzed cycloisomerization of 1.

Condition A. IPr-GaCl₃ (5 mol %, 0.0125 mmol, 7.06 mg) was dissolved in DCE (0.5 mL) in a screw-cap vial under argon. [Ag][Al(pftb)₄] (7 mol %, 0.0175 mmol, 18.81 mg) was added, and the mixture was stirred for 5 min. A solution of enyne 1 (0.25 mmol, 59.6 mg) in DCE (0.5 mL) was added and the reaction mixture was

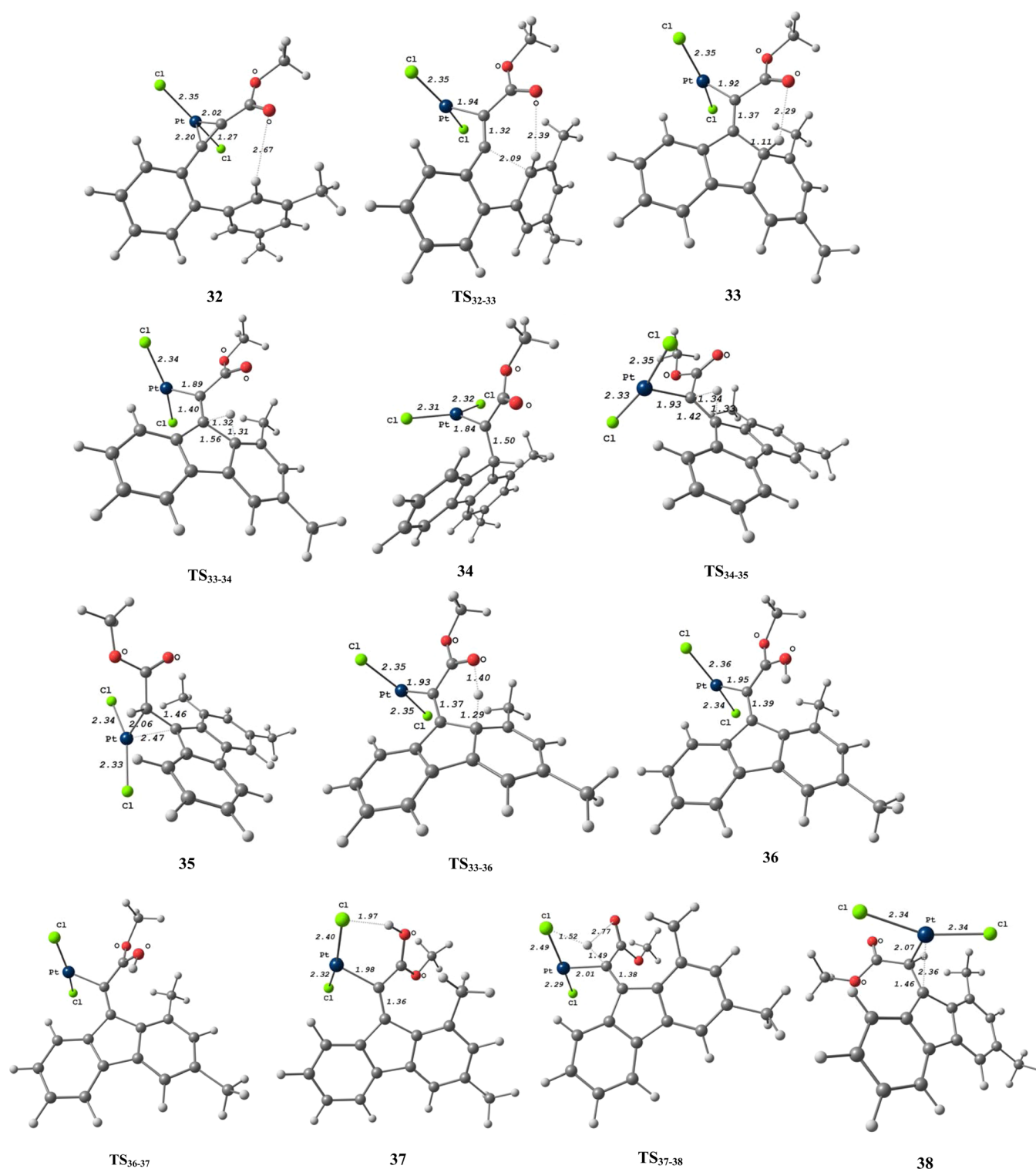


Figure 5. Geometries of the computed species shown in Scheme 13 (distances in Å).

stirred at 80 °C for 4 h. After filtration over a short pad of Celite and evaporation of the solvent, the crude residue was purified by chromatography over silica gel (10% AcOEt in pentane) to afford a mixture of **1**, **2-E**, and **2-Z** (21 mg) in 32% corrected yield of **2**. The ratio indicated in Table 4 was determined by GC. 97% conversion was determined based on the recovery of 3% of **1**.

Condition B. IPr-InBr₃ (5 mol %, 0.0125 mmol, 9.31 mg) was dissolved in DCE (0.5 mL) in a screw-cap vial under argon. [Ag][Al(pftb)₄] (7 mol %, 0.0175 mmol, 18.81 mg) was added, and the mixture was stirred for 5 min. A solution of enyne **1** (0.25 mmol, 59.6 mg) in DCE (0.5 mL) was

added, and the reaction mixture was stirred at 80 °C for 2 h. After filtration over a short pad of Celite and evaporation of the solvent, the crude residue was purified by chromatography over silica gel (10% AcOEt in pentane) to afford a mixture of **1**, **2-E**, and **2-Z** (30 mg) in 42% corrected yield of **2**. The ratio indicated in Table 4 was determined by GC. 92% conversion was determined based on the recovery of 8% of **1**.

Condition C. Ph₃PAuCl (5 mol %, 0.0125 mmol, 6.18 mg) was dissolved in DCE (0.5 mL) in a screw-cap vial under argon. AgSbF₆ (7 mol %, 0.0175 mmol, 6.01 mg) was added, and the mixture was stirred for 5 min. A solution of enyne **1** (0.25 mmol, 59.6 mg) in DCE (0.5 mL) was

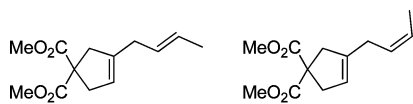
Table 4. Ratio of Enyne 1 and Dienes 2-E and 2-Z Determined by GC Analysis^a

condition	1 (area%)	2-E (area%)	2-Z (area%)	ratio (1: 2-E: 2-Z)
A	9.87	78.45	11.68	1:8: 1
B	15.26	69.66	15.08	1:4: 1
C	0	81.35	18.65	0:4: 1

^aMethod: 50 °C (1 min), slope 10 °C·min⁻¹ (20 min), 250 °C (2 min). GC retention time: 9.9 min (1), 10.9 min (2-E), 11.1 min (2-Z).

was added, and the reaction mixture was stirred at room temperature for 1 h. After filtration over a short pad of Celite and evaporation of the solvent, the crude residue was purified by chromatography over silica gel (10% AcOEt in pentane) to afford a mixture of 2-E and 2-Z (30 mg) in 50% yield. The ratio indicated in Table 4 was determined by GC.

(E)-Dimethyl 3-(but-1-en-1-yl)cyclopent-3-ene-1,1-dicarboxylate and (Z)-Dimethyl 3-(but-1-en-1-yl)cyclopent-3-ene-1,1-dicarboxylate 2.



4 : 1

Obtained following condition B (Table 1, entry 2). Colorless oil; 2-E:2-Z = 4:1 determined by GLC analysis. NMR of the major isomer 2-E: ¹H NMR (360 MHz, CDCl₃) δ 5.52–5.38 (m, 2H), 5.22 (m, 1H), 5.10–5.19 (m, 2-Z), 3.73 (s, 8.4H, 2-E and 2-Z), 2.99 (m, 2.7H, 2-E and 2-Z), 2.92 (m, 2.7H, 2-E and 2-Z), 2.80–2.75 (m, 2-Z), 2.72 (m, 2H), 1.66 (d, J = 5.4 Hz, 3H), 1.61 (d, J = 6.5 Hz, 2-Z); ¹³C NMR (90 MHz, CDCl₃) δ 172.7, 140.9, 127.6, 126.7, 120.7, 59.0, 52.8, 43.0, 40.7, 33.9, 17.8; FT-IR (film): ν 1736, 1434, 1256, 1194, 1160, 1070, 966 cm⁻¹; HRMS (ESI) m/z: calcd for C₁₃H₁₈O₄Na [M + Na]⁺: 261.1097 found: 261.1095. The data correspond to those previously described in the literature.^{4a}

Procedure for the Hydroarylation of Arenyne 21. A solution of arenyne 21 (0.125 mmol, 36.8 mg) and anisole (0.75 mmol, 41 μL) in DCE or toluene (0.5 mL) was added to GaCl₃ (10 mol %, 0.0125 mmol, 2.2 mg) in a screw-cap vial under argon. The reaction mixture was stirred at 80 °C for 2 h (full conversion was observed by TLC monitoring). After filtration over a short pad of silica gel (CH₂Cl₂), solvents were evaporated under vacuum. The yield of 22 was then determined by ¹H NMR analysis after the addition of 1 equiv of p-anisaldehyde (0.125 mmol, 15.2 μL) as internal standard. 54% of 22 was obtained when the reaction was performed in DCE, and 87% of 22 was obtained when the reaction was performed in toluene. The Friedel–Crafts adduct 23 was not observed in either case.

■ ASSOCIATED CONTENT

● Supporting Information

The Supporting Information is available free of charge on the ACS Publications website at DOI: 10.1021/acs.joc.5b02052.

NMR spectra of 2, energies and coordinates of the computed intermediates (PDF)

■ AUTHOR INFORMATION

Corresponding Author

*E-mail: vincent.gandon@u-psud.fr.

Notes

The authors declare no competing financial interest.

■ ACKNOWLEDGMENTS

This work was supported by UPS, IUF, and CNRS. We used the computing facility of the CRIHAN (project 2006-013)

■ REFERENCES

(1) Jung, M. E.; Piizzi, G. *Chem. Rev.* **2005**, *105*, 1735.

- (2) (a) Michelet, V.; Toullec, P. Y.; Genêt, J.-P. *Angew. Chem., Int. Ed.* **2008**, *47*, 4268. (b) Herrero-Gómez, E.; Echavarren, A. M. In *Handbook of Cyclization Reactions*, Shengming, M. Ed.; Wiley-VCH: Weinheim, Germany, 2010; Vol. 2, p 625. (c) Aubert, C.; Fensterbank, L.; Garcia, P.; Malacria, M.; Simonneau, A. *Chem. Rev.* **2011**, *111*, 1954. (d) Yamamoto, Y. *Chem. Rev.* **2012**, *112*, 4736. (e) Michelet, V. In *Comprehensive Organic Synthesis*, 2nd ed.; Knochel, P., Molander, G. A., Eds.; Elsevier: Amsterdam, The Netherlands, **2014**; Vol. 5, p 1483.10.1016/B978-0-08-097742-3.00531-0
- (3) (a) Inoue, H.; Chatani, N.; Murai, S. *J. Org. Chem.* **2002**, *67*, 1414. (b) Chatani, N.; Inoue, H.; Kotsuma, T.; Murai, S. *J. Am. Chem. Soc.* **2002**, *124*, 10294. (c) Mamane, V.; Hannen, P.; Fürstner, A. *Chem. - Eur. J.* **2004**, *10*, 4556. (d) Simmons, E. M.; Sarpong, R. *Org. Lett.* **2006**, *8*, 2883.
- (4) (a) Zhuo, L.-G.; Zhang, J.-J.; Yu, Z.-X. *J. Org. Chem.* **2012**, *77*, 8527. (b) Zhuo, L.-G.; Zhang, J.-J.; Yu, Z.-X. *J. Org. Chem.* **2014**, *79*, 3809. (c) Zhuo, L.-G.; Shi, Y.-C.; Yu, Z.-X. *Asian J. Org. Chem.* **2014**, *3*, 842.
- (5) Miyahana, Y.; Chatani, N. *Org. Lett.* **2006**, *8*, 2155.
- (6) The values presented here come from the Supporting Information of ref 4c. They are different from those presented in the article. Surprisingly the authors did not use the free energy values of their most stable isomers. Also the depicted transition states do not always correspond to the discussed series. By using the right values, we reached the same conclusions nonetheless.
- (7) The reaction of dimethyl cyclopropane-1,1-dicarboxylate with GaCl₃ yields the expected molecular adduct with no ionization of the Ga–Cl bond: Novikov, R. A.; Balakirev, D. O.; Timofeev, V. P.; Tomilov, Y. V. *Organometallics* **2012**, *31*, 8627. ⁷¹Ga NMR did not reveal the typical sharp signal of GaCl₄⁻.
- (8) (a) Li, H.-J.; Guillot, R.; Gandon, V. *J. Org. Chem.* **2010**, *75*, 8435. (b) Michelet, B.; Bour, C.; Gandon, V. *Chem. - Eur. J.* **2014**, *20*, 14488. (c) Michelet, B.; Colard-Itté, J.-R.; Thiery, G.; Guillot, R.; Bour, C.; Gandon, V. *Chem. Commun.* **2015**, *51*, 7401 and references cited therein.
- (9) Cycloisomerization of 1 into dienes under transition-metal catalysis has been reported twice but products 2 and 3 were not observed: (a) Kezuka, S.; Okado, T.; Niou, E.; Takeuchi, R. *Org. Lett.* **2005**, *7*, 1711. (b) Kondo, T.; Suzuki, N.; Okada, T.; Mitsudo, T.-a. *J. Am. Chem. Soc.* **1997**, *119*, 6187.
- (10) Hashmi, A. S. K.; Hutchings, G. J. *Angew. Chem., Int. Ed.* **2006**, *45*, 7896.
- (11) Since [Al(pftb)₄] is one of the most weakly coordinating anions, it is unlikely to interfere in the reaction process. See: Krossing, I. *Chem. - Eur. J.* **2001**, *7*, 490.
- (12) Häller, L. J. L.; MacGregor, S. A.; Panetier, J. A. In *N-Heterocyclic Carbenes: From Laboratory Curiosities to Efficient Synthetic Tools*, RSC Catalysis Series; Díez-González, S. Ed.; Royal Society of Chemistry: London, 2011; pp 42–76.
- (13) Zhao, Y.; Truhlar, D. G. *Theor. Chem. Acc.* **2008**, *120*, 215.
- (14) It should be difficult to synthesize, and the reaction products difficult to separate from the substrate.
- (15) Only the most stable isomer is presented in each case.
- (16) See inter alia: Olah, G. A.; Farooq, O.; Farnia, S. M. F.; Olah, J. A. *J. Am. Chem. Soc.* **1988**, *110*, 2560.
- (17) See inter alia: Matuszek, K.; Chrobok, A.; Hogg, J. M.; Coleman, F.; Swadźba-Kwaśny, M. *Green Chem.* **2015**, *17*, 4255 and the references therein.
- (18) (a) Tarakeshwar, P.; Lee, J. Y.; Kim, K. S. *J. Phys. Chem. A* **1998**, *102*, 2253. (b) Volkov, A. N.; Timoshkin, A. Y.; Suvorov, A. V. *Int. J. Quantum Chem.* **2004**, *100*, 412. (c) Volkov, A. N.; Timoshkin, A. Y.; Suvorov, A. V. *Int. J. Quantum Chem.* **2005**, *104*, 256. (d) Yamabe, S.; Yamazaki, S. *J. Phys. Org. Chem.* **2009**, *22*, 1094.
- (19) Soriano, E.; Marco-Contelles, J. *Organometallics* **2006**, *25*, 4542.
- (20) Computations on the gold(I)-phosphine-catalyzed hydroamination of alkynes suggest that the protodemetalation step is best achieved through a carbonyl relay, see: Kovács, G.; Ujaque, G.; Lledós, A. *J. Am. Chem. Soc.* **2008**, *130*, 853.
- (21) The use of additives (such as phthalimide or pyridine N-oxide) that have high hydrogen-bond basicity accelerates the protodemetalation step

in gold catalysis by proton shuttling, see: Wang, W.; Kumar, G. B.; Xu, B. *Org. Lett.* **2014**, *16*, 636.

(22) For computed *s*-alkane AlCl_3 complexes: Shilina, M. I.; Smirnov, V. V.; Bakharev, R. V. *Russ. Chem. Bull.* **2009**, *58* (S8), 675.

(23) Koleva, G.; Galabov, B.; Kong, J.; Schaefer, H. F., III; Schleyer, P. v. R. *J. Am. Chem. Soc.* **2011**, *133*, 19094.

(24) Galabov, B.; Koleva, G.; Kong, J.; Schaefer, H. F., III; Schleyer, P. v. R. *Eur. J. Org. Chem.* **2014**, *2014*, 6918.

(25) This value is much lower than that found with *gem*- CO_2Me in the tether (17.7 kcal/mol). This is an effect of the solvation. Without solvent correction, these values are very close: 33.9 and 34.4 respectively.

(26) Mamane, V.; Hannen, P.; Fürstner, A. *Chem. - Eur. J.* **2004**, *10*, 4556.

(27) (a) Balcells, D.; Clot, E.; Eisenstein, O. *Chem. Rev.* **2010**, *110*, 749. (b) Rousseaux, S.; Gorelsky, S. I.; Chung, B. K. W.; Fagnou, K. *J. Am. Chem. Soc.* **2010**, *132*, 10692.

(28) Frisch, M. J.; Trucks, G. W.; Schlegel, H. B.; Scuseria, G. E.; Robb, M. A.; Cheeseman, J. R.; Scalmani, G.; Barone, V.; Mennucci, B.; Petersson, G. A.; Nakatsuji, H.; Caricato, M.; Li, X.; Hratchian, H. P.; Izmaylov, A. F.; Bloino, J.; Zheng, G.; Sonnenberg, J. L.; Hada, M.; Ehara, M.; Toyota, K.; Fukuda, R.; Hasegawa, J.; Ishida, M.; Nakajima, T.; Honda, Y.; Kitao, O.; Nakai, H.; Vreven, T.; Montgomery, J. A., Jr.; Peralta, J. E.; Ogliaro, F.; Bearpark, M.; Heyd, J. J.; Brothers, E.; Kudin, K. N.; Staroverov, V. N.; Kobayashi, R.; Normand, J.; Raghavachari, K.; Rendell, A.; Burant, J. C.; Iyengar, S. S.; Tomasi, J.; Cossi, M.; Rega, N.; Millam, J. M.; Klene, M.; Knox, J. E.; Cross, J. B.; Bakken, V.; Adamo, C.; Jaramillo, J.; Gomperts, R.; Stratmann, R. E.; Yazyev, O.; Austin, A. J.; Cammi, R.; Pomelli, C.; Ochterski, J. W.; Martin, R. L.; Morokuma, K.; Zakrzewski, V. G.; Voth, G. A.; Salvador, P.; Dannenberg, J. J.; Dapprich, S.; Daniels, A. D.; Farkas, Ö.; Foresman, J. B.; Ortiz, J. V.; Cioslowski, J.; Fox, D. J. *Gaussian 09*, Revision D.01; Gaussian, Inc., Wallingford, CT, 2009.

(29) Zhao, Y.; Truhlar, D. G. The M06 Suite of Density Functionals for Main Group Thermochemistry, Thermochemical Kinetics, Non-covalent Interactions, Excited States, and Transition Elements. *Theor. Chem. Acc.* **2008**, *120*, 215–241.

(30) (a) Hariharan, P. C.; Pople, J. A. *Theoret. Chimica Acta* **1973**, *28*, 213. (b) Frantl, M. M.; Petro, W. J.; Hehre, W. J.; Binkley, J. S.; Gordon, M. S.; DeFrees, D. J.; Pople, J. A. *J. Chem. Phys.* **1982**, *77*, 3654. (c) Rassolov, V.; Pople, J. A.; Ratner, M.; Windus, T. L. *J. Chem. Phys.* **1998**, *109*, 1223.

(31) (a) Hay, P. J.; Wadt, W. R. *J. Chem. Phys.* **1985**, *82*, 270. (b) Hay, P. J.; Wadt, W. R. *J. Chem. Phys.* **1985**, *82*, 284. (c) Hay, P. J.; Wadt, W. R. *J. Chem. Phys.* **1985**, *82*, 299.

(32) (a) Barone, V.; Cossi, M. *J. Phys. Chem. A* **1998**, *102*, 1995. (b) Cossi, M.; Rega, N.; Scalmani, G.; Barone, V. *J. Comput. Chem.* **2003**, *24*, 669.

(33) (a) Lee, C.; Yang, W.; Parr, R. *Phys. Rev. B: Condens. Matter Mater. Phys.* **1988**, *37*, 785. (b) Becke, A. J. *J. Chem. Phys.* **1993**, *98*, 5648.

(34) Bergner, A.; Dolg, M.; Kuechle, W.; Stoll, H.; Preuss, H. *Mol. Phys.* **1993**, *80*, 1431.

(35) Marion, N.; Escudero-Adán, E. C.; Benet-Buchholz, J.; Stevens, E. D.; Fensterbank, L.; Malacria, M.; Nolan, S. P. *Organometallics* **2007**, *26*, 3256.

(36) Baker, R. J.; Davies, A. J.; Jones, C.; Kloth, M. *J. Organomet. Chem.* **2002**, *656*, 203.